

ActionCodec: What Makes for Good Action Tokenizers

Zibin Dong ^{*123} Yicheng Liu ^{*2} Shiduo Zhang ⁴⁵ Baijun Ye ² Yifu Yuan ³ Fei Ni ³ Jingjing Gong ⁵
Xipeng Qiu ⁵⁴ Hang Zhao ² Yinchuan Li ¹ Jianye Hao ³

Abstract

Vision-Language-Action (VLA) models leveraging the native autoregressive paradigm of Vision-Language Models (VLMs) have demonstrated superior instruction-following and training efficiency. Central to this paradigm is action tokenization, yet its design has primarily focused on reconstruction fidelity, failing to address its direct impact on VLA optimization. Consequently, the fundamental question of *what makes for good action tokenizers* remains unanswered. In this paper, we bridge this gap by establishing design principles specifically from the perspective of VLA optimization. We identify a set of best practices based on information-theoretic insights, including maximized temporal token overlap, minimized vocabulary redundancy, enhanced multimodal mutual information, and token independence. Guided by these principles, we introduce **ActionCodec**, a high-performance action tokenizer that significantly enhances both training efficiency and VLA performance across diverse simulation and real-world benchmarks. Notably, on LIBERO, a SmoVLM2-2.2B fine-tuned with ActionCodec achieves a 95.5% success rate without any robotics pre-training. With advanced architectural enhancements, this reaches 97.4%, representing a new SOTA for VLA models without robotics pre-training. We believe our established design principles, alongside the released model, will provide a clear roadmap for the community to develop more effective action tokenizers.

1. Introduction

Vision-Language-Action (VLA) models, which fine-tune Vision-Language Models (VLMs) on large-scale robotic

^{*}Equal contribution ¹Knowin AI (Work done during an internship) ²Tsinghua University ³Tianjin University ⁴Fudan University ⁵Shanghai Innovation Institute. Correspondence to: Hang Zhao <hangzhao@mail.tsinghua.edu.cn>, Jianye Hao <jianye.hao@tju.edu.cn>.

Preprint. February 18, 2026.

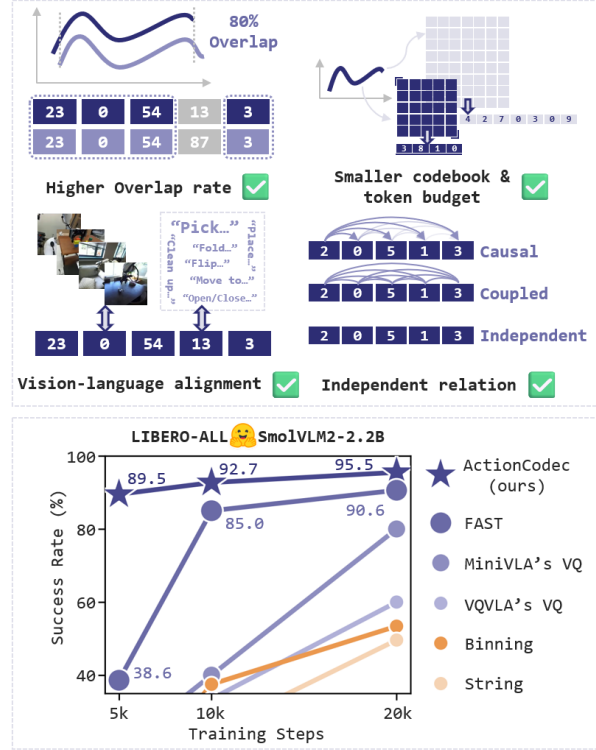


Figure 1. **ActionCodec** provides a comprehensive analysis of the VQ action tokenizer design elements that directly impact VLA training and summarizes the best practices. When utilized for the autoregressive fine-tuning of SmoVLM2-2.2B without additional architectural designs, ActionCodec achieves performance on the LIBERO benchmark that far exceeds other action tokenizers, particularly in terms of training efficiency.

interaction datasets, have emerged as a cornerstone for general-purpose physical intelligence (Driess et al., 2023; Zitkovich et al., 2023; Bai et al., 2024). While derived from VLMs, contemporary VLA architectures often diverge from the standard autoregressive paradigm by employing specialized action heads (Kim et al., 2025; Bu et al., 2025) or external diffusion-based experts (Black et al., 2024; Intelligence et al., 2025b). Recent evidence suggests that adhering to the native VLM generative framework, representing actions as discrete tokens, is crucial for preserving pre-trained general knowledge and fostering superior instruction-following capabilities (Driess et al., 2025; Intelligence et al., 2025a; Hancock et al., 2025; Zhang et al., 2025; Dong et al., 2025).

This trend is exemplified by state-of-the-art (SOTA) models like $\pi_{0.5}$ (Intelligence et al., 2025b), where discretized action tokens are central to the fine-tuning task. Consequently, the design of an effective action tokenization scheme has become a critical bottleneck in VLA research.

Existing action tokenizers generally fall into three categories: (1) Heuristic methods, which directly discretize signals into bins or raw strings (Kim et al., 2024; Goyal et al., 2025); (2) Semi-data-driven methods, which apply Byte-Pair Encoding (BPE) to frequency-domain signals (Pertsch et al., 2025); and (3) Data-driven methods, primarily based on Vector Quantization (VQ) to learn latent discrete representations (Wang et al., 2025b). Although VQ-based approaches are theoretically superior due to their minimal reliance on heuristic priors, they have historically lagged behind simpler schemes in downstream robotic tasks. We attribute this discrepancy to a fundamental research gap: existing literature evaluates VQ tokenizers through the lens of generative fidelity (e.g., reconstruction error), neglecting the complex training dynamics of the VLA backbone.

In this paper, we address the foundational question: *What makes for good action tokenizers* for VLA optimization? Moving beyond standard generative metrics, we analyze VLA performance through the prisms of information theory and representation learning. We identify four key desiderata for high-performance action tokens: (i) maximized temporal overlap between adjacent chunks, (ii) minimized vocabulary redundancy, (iii) enhanced mutual information between tokens and multimodal contexts, and (iv) token independence.

Guided by these principles, we introduce **ActionCodec**, a robust action tokenizer that integrates the identified optimal design choices. Moreover, ActionCodec leverages Residual Vector Quantization (RVQ) (Lee et al., 2022) post-training to refine reconstruction fidelity and incorporates embodiment-specific soft prompts to facilitate knowledge transfer across diverse robotic platforms. Our empirical results demonstrate that VLA models equipped with ActionCodec, without any additional architectural modifications, achieve unprecedented improvements in training efficiency, success rates, and anti-overfitting resilience across diverse benchmarks. ActionCodec achieves SOTA performance in both simulated and real-world environments, providing a systematic roadmap for the future of VQ-based action representation. Our contributions are summarized as follows:

- We establish a rigorous analytical framework to delineate the optimal design desiderata for action tokenization from the perspective of VLA training dynamics, providing a systematic roadmap for future research in general-purpose physical intelligence.
- We introduce **ActionCodec**, a high-performance action tokenizer that instantiates these validated principles.

ActionCodec substantially enhances the VLA training efficiency and mitigates overfitting.

- We provide a comprehensive suite of ActionCodec-powered VLA models across diverse architectural paradigms. Our approach achieves SOTA performance on multiple simulated and real-world benchmarks, demonstrating remarkable efficacy even when initialized from general VLMs without robotics pre-training.

2. Related Works

Vision-Language-Action Models. VLAs leverage the representational power of pre-trained VLMs to map visual observations and language instructions into robotic control signals (Driess et al., 2023; Zitkovich et al., 2023). Current VLA architectures primarily diverge in their action representation, falling into either continuous or discrete prediction frameworks. Continuous frameworks often necessitate structural deviations from the VLM’s native architecture, such as regressing actions from hidden states or integrating auxiliary generative experts such as diffusion or flow-matching models (Black et al., 2024; Shukor et al., 2025; Bjorck et al., 2025; Kim et al., 2025). Conversely, discrete frameworks discretize action spaces into tokens, enabling the model to utilize the standard autoregressive objective (Wang et al., 2025b; Goyal et al., 2025). While discrete methods may introduce higher sequential latency, they demonstrate a superior ability to preserve the VLM’s world knowledge and instruction-following capabilities (Liu et al., 2025). Notably, even SOTA heterogeneous models have recently integrated discrete action tokenization as an auxiliary task to improve performance (Driess et al., 2025; Intelligence et al., 2025b). This convergence underscores the pivotal role of action tokenization in the VLA design space.

Action Tokenization Schemes. The methodology for action discretization varies significantly. Early approaches employed uniform quantization (binning) of temporal signals (Kim et al., 2024; Lee et al., 2025), which often suffers from low training efficiency and ignores the inherent structure of the action space. Subsequent refinements, such as parallel decoding (Kim et al., 2025) or string-based token representation (Goyal et al., 2025), attempt to mitigate these issues but do not address the fundamental inefficiencies of heuristic binning. Other studies have attempted to represent actions as strings for direct VLM prediction (Hancock et al., 2025); however, this approach offers no significant performance benefits while greatly increasing the token budget and extending latency to several seconds, limiting real-world applicability. FAST (Pertsch et al., 2025) introduces Byte-Pair Encoding (BPE) on frequency-domain signals; however, its reliance on fixed geometric priors limits its capacity for cross-embodiment knowledge transfer. Data-driven schemes, particularly those based on Vector

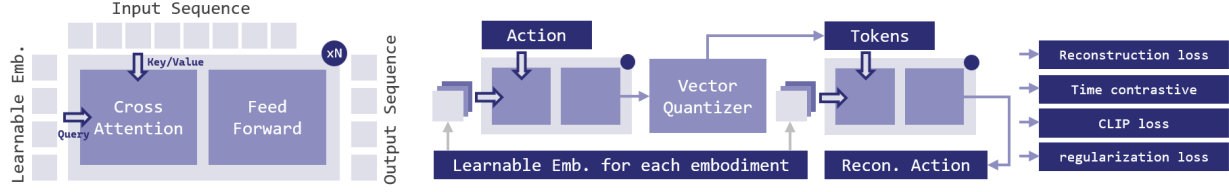


Figure 2. Neural Network Architecture of ActionCodec. We employ a Perceiver-like transformer architecture due to its inherent flexibility, which facilitates the modeling of diverse token relations and supports the encoding of variable-length action sequences.

Quantization (VQ) (Wang et al., 2025b; Belkhale & Sadigh, 2024; Mete et al., 2024; Lee et al., 2024), offer a more flexible alternative by learning discrete latent representations. Despite their potential, existing VQ-based tokenizers are often treated as black-box components. There remains a critical lack of understanding regarding the specific VQ properties that facilitate or obstruct VLA optimization, a gap that this work aims to bridge.

3. Preliminaries

We consider learning a policy $\pi_\theta(A|V, L)$ that maps visual observations V and language instructions L to an action sequence $A \in \mathbb{R}^{T \times D}$. To leverage the autoregressive paradigm of pre-trained VLMs, A is discretized into a proxy sequence of tokens $C = [c_1, c_2, \dots, c_n]$, where each c_k belongs to a vocabulary $\mathcal{K} = \{1, \dots, S\}$. This process is facilitated by a Vector Quantized (VQ) (van den Oord et al., 2017) tokenizer comprising an encoder \mathcal{F} and a decoder \mathcal{G} . Specifically, \mathcal{F} maps A to a continuous latent representation $Z = [z_1, \dots, z_n] \in \mathbb{R}^{n \times d}$, which is then quantized against a learnable codebook $\mathcal{B} = \{e_j\}_{j=1}^S \subset \mathbb{R}^d$ such that $c_k = \arg \min_{j \in \{1, \dots, S\}} \|z_k - e_j\|_2$. The reconstructed action sequence is denoted as $\hat{A} = \mathcal{G}(e_{c_1}, \dots, e_{c_n})$. The tokenizer is optimized via

$$\mathcal{L}_{VQ} = \|A - \hat{A}\|_2^2 + \|\text{sg}[Z] - e_c\|_2^2 + \|Z - \text{sg}[e_c]\|_2^2, \quad (1)$$

where $\text{sg}[\cdot]$ is the stop-gradient operator.

4. A VLA Perspective on Action Tokenization

We formalize action tokenization as the construction of an optimal proxy target for VLA optimization. Since the tokenizer dictates the target distribution, VLA training involves both model fitting and the implicit optimization of the supervision signal. The expected negative log-likelihood (NLL) loss is decomposed as:

$$\mathbb{E}[\mathcal{L}_{\text{NLL}}] = D_{KL}(P_{\text{data}} \parallel P_\theta) + H(C|V, L), \quad (2)$$

where the conditional entropy $H(C|V, L)$ quantifies the *supervisory ambiguity*. High entropy induces conflicting gradients, forcing the model to fit stochastic noise rather than underlying physics. Minimizing this term is equivalent

to denoising the training objective. By leveraging the definition of mutual information, we decompose this entropy into three components:

$$H(C|V, L) = \underbrace{H(C|A)}_{\text{Artifact Entropy}} + \underbrace{I(C; A)}_{\text{Capacity}} - \underbrace{I(C; V, L)}_{\text{Perceptual Alignment}} \quad (3)$$

Guided by Equation (3), we identify three critical metrics for an optimal tokenizer: **(a) Overlap Rate.** Artifact entropy $H(C|A)$ measures the topological instability of the tokenizer (Section D), where minor action perturbations (e.g., sensor noise) trigger stochastic jumps in token space. Stability is achieved by ensuring C remains consistent across temporally overlapping action chunks (A_t and A_{t+1}). We quantify this via the *overlap rate* between adjacent chunks; a higher rate implies a more stable supervision signal. **(b) Capacity and Vocabulary Size.** The term $I(C; A)$ represents the information bottleneck. Assuming suppressed artifact entropy, this term is upper-bounded by the marginal entropy: $I(C; A) \approx H(C) \leq \sum_{k=1}^n H(c_k) \leq n \log_2 S$. This bound is jointly determined by the token budget n and vocabulary size S . While sufficient capacity is required for reconstruction, excessive capacity encodes high-frequency noise. Reducing n and S simplifies the learning manifold for the VLA. **(c) Perceptual Alignment vs. Residual Grammar.** To understand the information sources utilized for prediction, we decouple the total information gain for a token c_k using the chain rule:

$$I(c_k; V, L, c_{<k}) = \underbrace{I(c_k; V, L)}_{\text{Total Information}} + \underbrace{I(c_k; c_{<k}|V, L)}_{\text{Visual-Language Alignment} + \text{Residual Grammar}} \quad (4)$$

Visual-Language alignment measures the direct correlation between tokens and multimodal inputs, while *residual grammar* quantifies the dependency on autoregressive history given the context. An effective tokenizer must balance these pathways to prevent the model from over-relying on temporal priors at the expense of environmental grounding.

Guided by these principles, the subsequent sections show the derivation of best practices for VQ-based tokenization, starting from a vanilla VQ-VAE architecture (Figure 2) trained on the LIBERO (Liu et al., 2024) dataset as an empirical foundation. To validate the efficacy of these design choices, we move beyond intrinsic reconstruction metrics and directly fine-tune SmolVLM2-256M (Marafioti et al., 2025)

as a VLA model. The quality of the tokenization scheme is thus measured by the resulting policy’s performance on the LIBERO-Goal benchmark (refer to Section A.2 for comprehensive experimental settings).

4.1. Impacts of Overlap Rate

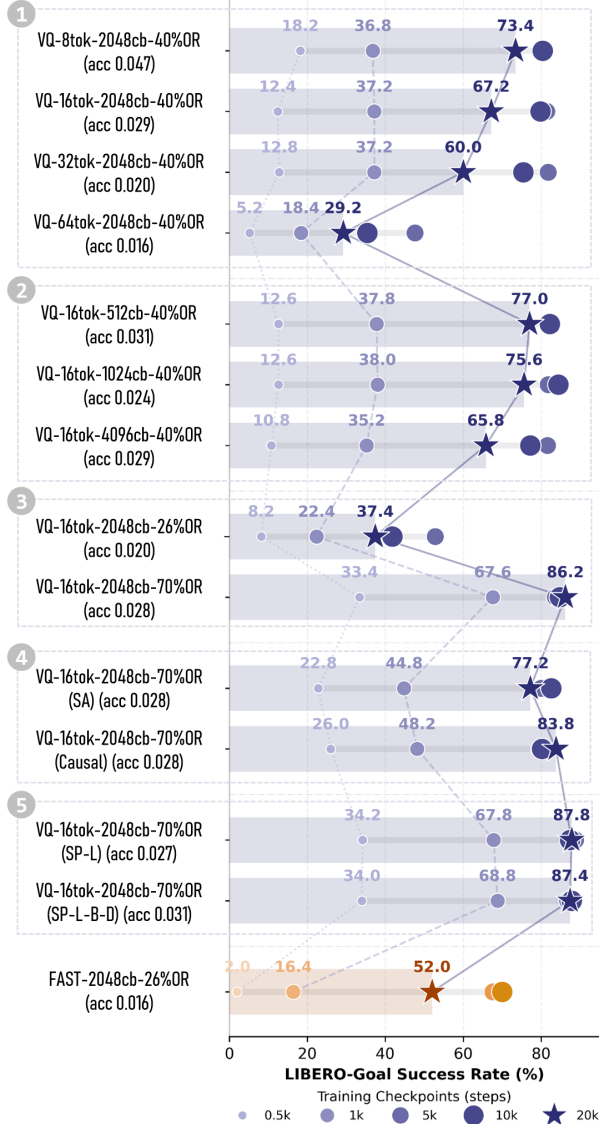


Figure 3. LIBERO-Goal results for different design choices. All VLA models are based on the SmolVLM2-256M backbone, following vocabulary expansion and full-parameter fine-tuning without additional architectural modifications. The suffix notations are defined as follows: acc (L1 reconstruction error), tok (token budget), cb (vocabulary size), OR (overlap rate), SA (self-attention), Causal (SA w/ causal mask), and SP (training w/ soft-prompt).

To investigate the effects of the overlap rate (OR) on VLA optimization, we synthesize three tokenizer variants with controlled OR levels (26%, 40%, and 70%) by augmenting the VQ-VAE objective with a contrastive loss to modulate

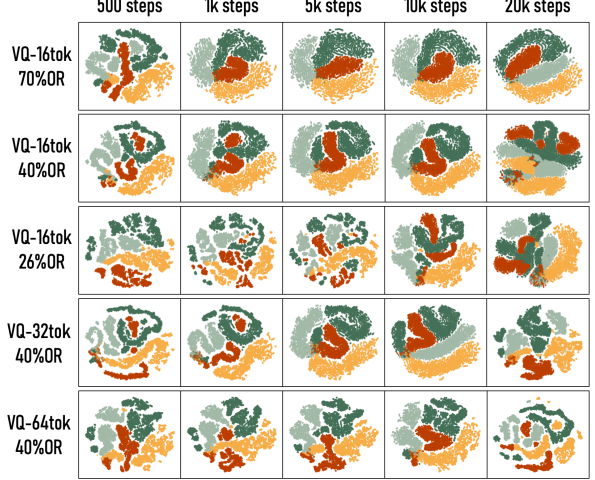


Figure 4. t-SNE visualization of the VLA’s last hidden states for the action [BOS] token on four LIBERO-Goal tasks.

the topological stability of the token space. The performance on LIBERO-Goal, summarized in Figure 3 (Block 1 & 3), demonstrates that a higher OR consistently enhances training efficiency, asymptotic convergence, and robustness. Notably, the 70% OR tokenizer enables the VLA to achieve a 33.4% success rate within a mere 500 training steps, significantly outperforming the naive VQ-VAE (8.2%) and the FAST baseline (2%). To further explore the underlying mechanism, we select data from four distinct tasks and visualize the last hidden states of the VLA’s action [BOS] token using t-SNE, as shown in the first three rows of Figure 4. The visualizations reveal that a high OR enables the VLA model to form distinct clusters in the latent space significantly earlier in the training process. Furthermore, these cluster distributions remain more stable over training time, effectively mitigating the risk of overfitting. Consequently, we establish maximizing the overlap rate as a primary design requirement for the action tokenizer.

4.2. Impacts of Vocabulary Size and Token Budget

As established in our theoretical framework, the capacity of the action proxy is governed by the entropy upper bound $n \log_2 S$. We evaluate various configurations spanning $n \in \{8, 16, 32, 64\}$ and $S \in \{512, 1024, 2048, 4096\}$ under a fixed OR to isolate their influence on optimization. Our results in Figure 3 (Blocks 1 & 2) indicate that these parameters primarily dictate the VLA’s resilience to overfitting, with the token budget n exerting a substantially more dominant influence than the vocabulary size S . A comparison across Rows 1, 4, and 5 of Figure 4 further elucidates this phenomenon: while an increased token budget n preserves sufficient task discriminability, it leads to excessive dispersion in the latent clusters. This expanded representational capacity makes the model increasingly susceptible to capturing high-frequency noise and spurious correlations.

Conversely, aggressive reduction of n and S eventually incurs a non-trivial reconstruction penalty, as the tokenizer fails to capture the necessary physical nuances of the action space. By navigating this trade-off between representational fidelity and the complexity of the learning manifold, we identify $S = 2048$ and $n = 16$ as a practical design choice.

4.3. Impacts of Vision-Language Alignment and Residual Grammar

Within the autoregressive framework, we decompose the token’s perceptual alignment into two competing information pathways: *visual-language alignment* $I(c_k; V, L)$, representing environmental grounding, and *residual grammar* $I(c_k; c_{<k}|V, L)$, quantifying autoregressive dependencies. To optimize the former, we integrate Time Contrastive Learning (TCL) and CLIP-based objectives into the tokenizer training:

$$\mathcal{L}_{\text{TCL}} = - \sum_i \log \frac{e^{S(Z^i, Z^{i+})}}{e^{S(Z^i, Z^{i+})} + e^{S(Z^i, Z^{i-})}}, \quad (5)$$

$$\mathcal{L}_{\text{CLIP}} = - \sum_i \sum_j \log \frac{1}{1 + e^{(l_{ij}(-tZ^i y^j + b))}}, \quad (6)$$

where Z^i , Z^{i+} , and Z^{i-} denote the continuous embeddings of the action chunk, its adjacent neighbor, and other action chunks within the batch, respectively; S denotes cosine similarity; y^j is the language embedding, l_{ij} is an indicator variable that equals 1 if i and j are paired and -1 otherwise, and t and b are learnable parameters. Additionally, an L_1 penalty regulation loss is applied to ensure training stability. Our findings are two-fold: **Differential effects of TCL and CLIP.** Visualizations of the VLA attention maps for the action [BOS] token (Figure 5, left) reveal that CLIP-trained tokenizers cause the VLA to focus on instruction-relevant objects, whereas TCL-trained tokenizers bias attention toward dataset-specific demonstration patterns (e.g., specific grasp points). (b) **Improved Overlap Rate and Structure.** Both objectives enhance the overlap rate and stability. As shown in the t-SNE visualizations of all 40 LIBERO tasks (Figure 5, right), TCL and CLIP training produces more structured latent clusters than simple action-perturbation methods. Thus, we adopt TCL and CLIP as the primary practices for improving OR.

Regarding **Residual Grammar**, we investigate whether inter-token dependencies aid VLA optimization by comparing Perceiver-based (independent tokens), Self-Attention (SA), and Causal-SA architectures. Surprisingly, while internal attention improves residual grammar, it degrades VLA performance by fostering an over-reliance on historical tokens. Perturbation experiments (Figure 6) demonstrate that independent tokens are significantly more robust; in contrast, Causal and SA structures are sensitive to early-sequence errors, leading to temporal hallucinations where the model

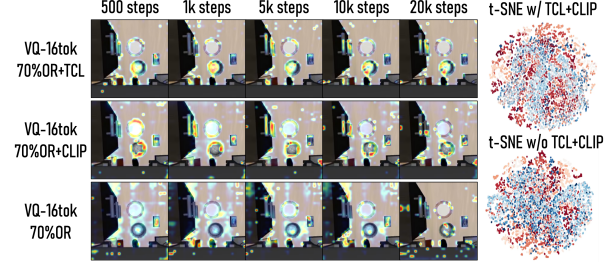


Figure 5. (Left) VLA attention maps for CLIP vs. TCL-trained tokenizers. (Right) t-SNE visualization of the structured latent space across 40 LIBERO tasks.

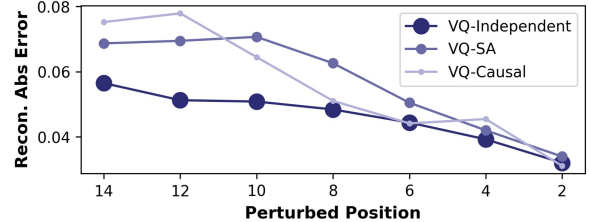


Figure 6. **Error propagation under token perturbation.** We measure the L1 reconstruction error when noise is injected at specific positions during generating. VQ-Independent maintains a stable, lower error compared to SA and Causal architectures. This justifies our design choice to decouple tokens and minimize residual grammar for more robust VLA optimization.

ignores real-time visual feedback. As shown in Figure 3 (Block 4), independent tokenization yields the highest task success rates and faster early-stage convergence. Thus, we advocate for a decoupled, independent tokenization scheme to maximize the VLA’s sensitivity to multimodal inputs.

5. ActionCodec

Synthesizing the aforementioned design principles, we introduce **ActionCodec**, a high-performance action tokenizer that instantiates the identified optimal design desiderata while incorporating the following practical enhancements.

Embodiment-specific Soft-prompts. To support multi-embodiment data integration and cross-platform knowledge transfer, we augment the Perceiver-based backbone with learnable *soft-prompt* embeddings. While global network parameters are shared to distill universal robotic priors, distinct soft-prompts are assigned to each embodiment to capture unique mechanical constraints and control frequencies. This hierarchical representational strategy enables ActionCodec to undergo effective large-scale pre-training across diverse datasets, including LIBERO (Liu et al., 2024), Bridge-Data (Walke et al., 2023), and DROID (Khazatsky et al., 2024). With a unified action latent space, we facilitate zero-shot action re-targeting and accelerate fine-tuning on novel robotic platforms. (See soft-prompts details in Section B.)

RVQ Post-training. While our analysis indicates that VLA optimization is robust to reconstruction errors below a



Figure 7. All evaluation benchmarks. We evaluate VLA models on 4 LIBERO task suites, Bridge-WidowX tasks on SimplerEnv, SO100-ShapeSorter tasks, and xArm tabletop manipulation tasks.

critical threshold, maximizing fidelity is essential for fine-grained manipulation. However, standard Residual Vector Quantization (RVQ) (Lee et al., 2022) typically achieves high fidelity at the expense of topological stability, often reducing the overlap rate (OR) to below 20%, which severely destabilizes VLA training. To resolve this trade-off, we propose an *RVQ post-training* phase. We first pre-train a single-layer VQ model to maximize OR and perceptual alignment, establishing a stable supervision manifold. Subsequently, we freeze the encoder and the primary codebook, introducing additional residual codebooks to minimize the remaining reconstruction error. It allows ActionCodec to refine action precision orthogonally to the token’s topological stability, ensuring zero degradation to VLA training efficiency while facilitating compatibility with advanced prediction paradigms such as Block-wise Autoregression (BAR) (Liu et al., 2025). (See RVQ details in Section C.)

6. Experiments

We evaluate **ActionCodec** across diverse benchmarks to address four key research questions: (i) Does ActionCodec outperform existing heuristic and data-driven tokenizers in efficiency and success rate? (ii) Can ActionCodec effectively integrate with and enhance prevailing VLA architectural paradigms? (iii) How does ActionCodec perform on real-world robotic platforms? (iv) What is the impact of specific design choices on the performance of ActionCodec?

6.1. Comparison with Mainstream Action Tokenizers

To facilitate a rigorous comparison, we integrate all evaluated action tokenizers into a unified VLA framework by expanding the vocabulary of the SmolVLM2-2.2B (Marafji

Table 1. LIBERO Benchmark Results. Comparison of success rates (%). **Pt.** denotes pre-trained VLA backbones. **Avg.**

Rank indicates relative performance across tasks. Best results in each block are **bolded**, second best are underlined.

Model	Pt.	Goal	Spatial	Object	Long	Avg.	Avg.-Rank
Octo-Base (27)	Y	84.6	78.9	85.7	51.1	75.1	10.5
SpatialVLA (30)	Y	78.6	88.2	89.9	55.5	78.1	9.5
GR00T-N1 (3)	Y	93.0	94.4	97.6	90.6	93.9	6.6
UniVLA (5)	Y	95.6	96.5	96.8	92.0	95.2	5.4
VQ-VLA (36)	Y	75.2	-	-	60.0	-	-
OpenVLA (18)	Y	79.2	84.7	88.4	53.7	76.5	10.0
OpenVLA-OFT (19)	Y	<u>97.9</u>	<u>97.6</u>	98.4	<u>94.5</u>	<u>97.1</u>	<u>2.5</u>
π_0 (4)	Y	95.8	96.8	98.8	85.2	94.2	4.5
$\pi_{0.5}$ (15)	Y	98.0	98.8	98.2	92.4	96.8	<u>2.5</u>
π_0 FAST (29)	Y	88.6	96.4	96.8	60.2	85.5	7.4
ActionCodec (2.2B)	N	95.4	96.2	<u>99.6</u>	90.6	95.5	5.1
ActionCodec-BAR	N	97.6	97.2	<u>99.8</u>	94.8	<u>97.4</u>	2.0
<hr/>							
Diffusion Policy (7)	N	68.3	78.3	92.5	50.5	72.4	13.8
MiniVLA (2)	N	-	-	-	77.0	-	-
OpenVLA-OFT (19)	N	91.7	94.3	95.2	86.5	91.9	7.8
SmolVLA 2.2B (31)	N	91.0	93.0	94.0	77.0	88.8	10.2
π_0 FAST (29)	N	89.0	87.0	63.0	48.0	71.8	14.2
$\pi_{0.5}$ (15)	N	94.6	96.6	97.2	85.8	93.3	6.4
VLA-0 (12)	N	96.2	<u>97.0</u>	97.8	87.6	94.7	3.8
<hr/>							
<i>SmolVLM2-2.2B (256M/500M) + Tokenizers</i>							
Binning	N	27.4	64.2	71.0	50.8	53.4	15.5
String	N	30.8	69.6	71.6	26.4	49.6	15.5
VQVLA’s	N	60.5	56.0	69.8	51.4	60.5	15.2
MiniVLA’s	N	82.1	82.8	90.2	75.2	82.6	12.8
FAST	N	89.2	90.2	97.2	85.8	90.6	9.4
ActionCodec (256M)	N	91.2	94.2	97.0	86.8	92.3	7.5
ActionCodec (500M)	N	96.4	91.6	96.0	85.8	92.5	7.8
ActionCodec (2.2B)	N	95.4	96.2	<u>99.6</u>	90.6	95.5	3.8
<hr/>							
<i>Variants</i>							
ActionCodec-PD	N	<u>97.0</u>	95.2	98.4	<u>91.6</u>	<u>95.6</u>	<u>3.0</u>
ActionCodec-KI	N	95.0	93.6	97.6	90.8	94.3	5.5
ActionCodec-BAR	N	97.6	97.2	99.8	94.8	97.4	1.0

oti et al., 2025) backbone and performing full-parameter autoregressive fine-tuning on the LIBERO benchmark. The detailed prompts utilized for these experiments are provided in Section A.3. We compare ActionCodec against several mainstream tokenization schemes: (i) **Binning**, which discretizes each action dimension into 1,000 uniform bins (Goyal et al., 2025); (ii) **String**, representing actions as raw text strings (Hancock et al., 2025); (iii) **VQ-based baselines** from MiniVLA (Belkhale & Sadigh, 2024) and VQ-VLA (Wang et al., 2025b); and (iv) the **FAST tokenizer** (Pertsch et al., 2025). Figure 1 illustrates the learning curves for each method, highlighting the exceptional training efficiency of our approach. ActionCodec not only achieves the highest peak success rate but also significantly outpaces all baselines in convergence speed; specifically, it attains an 89.5% success rate within a mere 5K training steps, while the runner-up (FAST) only achieves 38.6% at the same interval. Furthermore, ActionCodec exhibits remarkable scaling performance as detailed in the *SmolVLM2 (256M/500M)* section of Table 1: the performance of the 256M and 500M variants equipped with ActionCodec exceeds that of other tokenizers even when they utilize the much larger 2.2B VLM backbone. This suggests that the quality of the action

Table 2. SimplerWidowX Benchmark Results. Comparison of success rates (%). **Pt.** denotes pre-trained VLA backbones. **Avg. Rank** indicates relative performance across tasks. Best results in each block are **bolded**, second best are underlined.

Model	Pt.	Spoon	Carrot	Block	Eggplant	Avg.	Avg. Rank
Octo-Base (27)	Y	12.5	8.3	0.0	43.1	16.0	7.3
SpatialVLA (30)	Y	16.7	25.0	29.2	100.0	42.7	4.0
π_0 (4)	Y	<u>66.7</u>	58.3	58.3	<u>88.3</u>	67.9	2.0
OpenVLA-OFT (19)	Y	12.5	4.2	8.3	0.0	6.3	8.1
UniVLA (5)	Y	54.2	66.7	50.0	4.2	43.8	<u>3.5</u>
OpenVLA (18)	Y	32.0	30.0	18.0	38.0	29.5	4.8
VQ-VLA (36)	Y	12.5	8.0	6.0	0.0	6.6	8.1
π_0 FAST (29)	Y	29.1	21.9	10.8	66.6	32.1	5.3
ActionCodec-BAR	N	71.7	<u>64.2</u>	<u>55.0</u>	70.0	<u>65.2</u>	2.0
MiniVLA (2)	N	<u>68.0</u>	<u>44.0</u>	70.0	<u>14.0</u>	<u>49.0</u>	<u>1.8</u>
ActionCodec-BAR	N	71.7	64.2	<u>55.0</u>	70.0	65.2	1.3

Table 3. Action Tokenization Performance and Efficiency. Comparison of token budget, overlap rate (OR), and inference metrics. All models are evaluated on the LIBERO benchmark.

Tokenizer	Token Budget	OR	Horizon	Latency (s)	Throughput (action/s)	SR (%)
Binning (12)	140.0±0.0	39%	20	4.9	4.1	3.5
Binning (12)	56.0±0.0	38%	8	2.6	3.1	53.4
String (13)	779.2±17.3	28%	20	33.8	0.6	20.4
String (13)	311.8±7.8	34%	8	12.7	0.6	49.6
VQVLA's (36)	4.0±0.0	45%	5	0.7	7.7	60.5
MiniVLA's (2)	7.0±0.0	40%	8	0.7	11.1	82.6
FAST (29)	24.3±9.1	19%	20	1.5	13.1	90.6
ActionCodec	16.0±0.0	72%	20	0.9	22.0	95.5

representation is as critical as the scale of the VLM itself.

Finally, we evaluate throughput and latency in Table 3. Our analysis reveals that naive tokenization schemes, such as Binning and String, suffer from prohibitive latency and low throughput, rendering them impractical for real-time robotic deployment. In contrast, ActionCodec achieves the highest action throughput while maintaining superior task performance, establishing it as a robust and efficient solution for high-frequency closed-loop control.

6.2. Integration with Prevailing VLA Paradigms

To demonstrate the architectural versatility of ActionCodec, we evaluate its compatibility with three prevailing VLA paradigms: (i) **Parallel Decoding (PD)**, which employs an action expert with bidirectional attention to predict tokens in a single forward pass (Kim et al., 2025); (ii) **Knowledge Isolation (KI)**, which decouples the VLM’s semantic knowledge from action generation by using a diffusion action expert conditioned on the VLM’s KV cache (Intelligence et al., 2025b); and (iii) **Block-wise Autoregression (BAR)**, a hierarchical approach that utilizes RVQ to predict codebook levels in parallel while maintaining inter-block autoregressive dependencies (Liu et al., 2025). We provide more details in Section A.4.

As detailed in Table 1, ActionCodec seamlessly integrates with all three paradigms, consistently yielding performance gains. On the LIBERO benchmark, both PD and BAR

variants outperform the native autoregressive baseline. Notably, **ActionCodec-BAR** establishes a new SOTA for VLA models without robotics pre-training, achieving a 97.4% average success rate. Remarkably, this performance even surpasses several competitive models that benefit from extensive robotics pre-training. While the KI paradigm exhibits a slightly lower success rate compared to the autoregressive baseline, it outperforms its FAST-based counterpart—exemplified by $\pi_{0.5}$ without robotics pre-training. To further assess the zero-shot generalization and out-of-distribution (OOD) robustness of our approach, we conduct evaluations on the Simpler-WidowX benchmark (Table 2). ActionCodec-BAR maintains its dominant performance in this challenging setting, achieving the highest rank among all models trained with or without prior robotic data.

6.3. Real-world Evaluation

SO100-ShapeSorter. We design the SO100-ShapeSorter¹ task (Figure 7) to verify the efficacy of ActionCodec on low-cost robotic platforms and the advantages of large-scale data integration. This task requires the SO100 arm to insert blocks of specific numerical shapes into matching slots. Due to the high-precision requirements and the narrow tolerance of the slots, successful insertion is challenging even for human operators, who frequently require multiple corrective attempts. Consequently, our task-specific dataset is naturally rich in *recovery behaviors*, capturing the stochastic process of failure and re-adjustment. We evaluate the impact of co-training (CT) by comparing ActionCodec trained with 22.9K episodes of SO100 community data (Shukor et al., 2025) against a task-only variant (**ActionCodec w/o CT**), alongside baselines π_0 and π_0 FAST. As shown in Figure 8, while all models demonstrate reasonable picking capabilities, a significant performance gap emerges during the *Place* phase. Specifically, although the task-specific demonstrations contain recovery trajectories, the *w/o CT* variant fails to effectively model or reproduce these strategies during inference, often stalling after an initial misalignment. In contrast, the co-trained ActionCodec successfully leverages the broader representational prior to navigate the complex distribution of corrective actions. This enables the VLA to exhibit robust closed-loop recovery, such as re-aligning the block after a failed insertion attempt (Figure 9). These results underscore that while recovery data may be present in small-scale task datasets, the diverse priors provided by ActionCodec’s co-training are essential for the VLA to successfully internalize and execute these long-tail behaviors.

xArm-PickVeg. We design the xArm-PickVeg² task (Fig-

¹SO100 Dataset: <https://huggingface.co/datasets/zibinDong/actioncodec-so100-part1>

²xArm Dataset: https://huggingface.co/datasets/zibinDong/xarm_pickplace

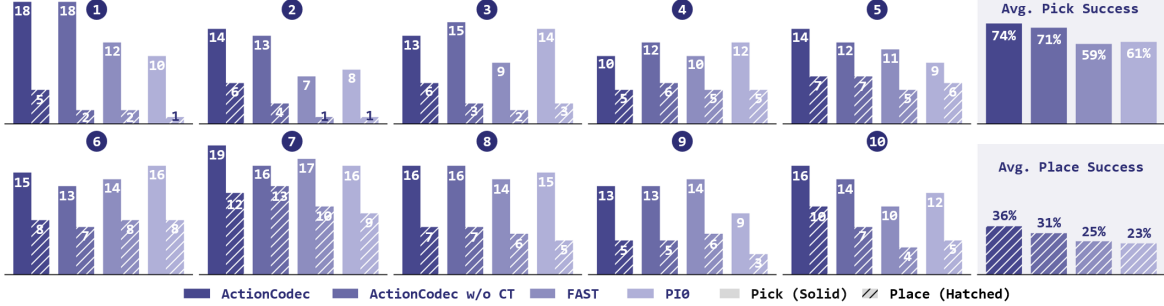


Figure 8. Success Rates on SO100-ShapeSorter. We report success counts for *Pick* (solid) and *Place* (hatched) across 10 tasks. While recovery actions are inherently present in our task demonstrations due to the difficulty of slot insertion, only **ActionCodec** (with CT) successfully learns to reproduce these corrective strategies. The performance gap is most prominent in the *Place* phase, where co-training facilitates the execution of complex, long-tail recovery behaviors that task-only models fail to capture.

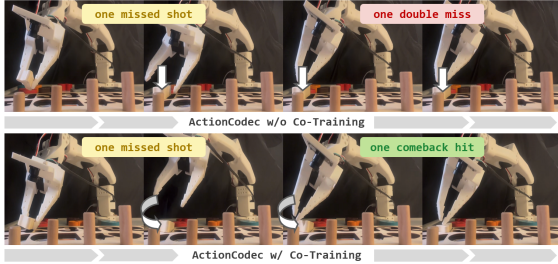


Figure 9. Comparison of recovery behaviors on SO100. After an initial missed shot, ActionCodec with co-training successfully executes a corrective adjustment to complete the insertion, whereas the variant without co-training stalls after a failure.

Table 4. Success Rates on xArm-PickVeg. ActionCodec w/ PT leverages heterogeneous priors to achieve the highest success rate.

Model	ActionCodec w/ PT	ActionCodec w/o PT	π_0	π_0 FAST
SR (%)	82.5	74.1	75.0	72.5

ure 7) to verify the efficacy of ActionCodec on high-performance robotic platforms and investigate the benefits of representational pre-training. We assess the transfer learning capabilities of ActionCodec under two distinct initialization regimes: (i) **w/ PT**, which utilizes weights pre-trained on large-scale heterogeneous datasets, and (ii) **w/o PT**, which employs standard randomized initialization. As illustrated by the optimization curves in Figure 13, the pre-trained variant (*w/ PT*) demonstrates superior optimization dynamics, exhibiting both lower L_2 reconstruction error and a higher OR compared to the *w/o PT* counterpart. This enhanced representational stability directly translates to improved downstream control performance. As summarized in Table 4, ActionCodec (*w/ PT*) achieves an 82.5% success rate (SR). These results underscore ActionCodec’s capacity for efficient fine-tuning and robust knowledge transfer when adapting to novel, high-performance robotic platforms.

Table 5. Ablations. We ablate various design choices for on LIBERO. We report the average success rate over the four suites.

ID	Co-Training	Soft Prompt	RVQ Post Training	VLM	LIBERO Avg.
0	✗	✗	✓	🟡	92.0 (-3.5%)
1	✓	✗	✓	🟡	92.7 (-2.8%)
2	✓	✓	✗	🟡	95.2 (-0.3%)
3	✓	✓	✓	🟡	95.5
4	✓	✓	✓	🟣	95.1
5	✓	✓	✓	🟣	94.6

6.4. Ablation Study

We conduct a series of ablation studies on the LIBERO benchmark. Table 5 summarizes these results.

Soft Prompts. Embodiment-specific soft prompts are vital for cross-platform knowledge transfer. Their omission (ID 1) reduces the benefits of diverse pre-training to marginal levels. Qualitative tests, transferring Bridge-WidowX actions to LIBERO-Franka, DROID-Franka, and xArm (Figure 10), reveal congruent motion trends, confirming that soft prompts enable a unified, platform-agnostic latent space. **RVQ Post-training.** While RVQ post-training further reduces reconstruction error, its impact on success rates is modest (ID 2 vs. 3). This validates that topological stability (OR) outweighs absolute fidelity during VLA optimization. **VLM Compatibility.** ActionCodec is backbone-agnostic, maintaining robust and comparable performance (IDs 3–5) across diverse architectures: 🟡 SmolVLM2-2.2B (Marafioti et al., 2025), 🟣 Qwen2.5VL-3B (Yang et al., 2025), and 🟤 InternVL3.5-2B (Wang et al., 2025a).

7. Conclusion

In this paper, we systematically analyze the critical design elements of action tokenization, leading to the introduction of **ActionCodec**. By integrating identified best practices, ActionCodec achieves superior performance across diverse simulation and real-world benchmarks. While currently pre-trained on a limited selection of large-scale robotic datasets, future work will focus on scaling these representations to achieve robust in-the-wild transfer across a broader vari-

ety of robotic embodiments. Furthermore, investigating optimized neural architectures and refined vision-language alignment schemes remains a promising direction. We believe both ActionCodec and the design principles established in this work provide a clear roadmap for the community to develop next-generation physical intelligence.

Impact Statement

This paper presents work whose goal is to advance the field of Machine Learning. There are many potential societal consequences of our work, none which we feel must be specifically highlighted here.

References

Bai, C., Xu, H., and Li, X. Embodied-ai with large models: research and challenges. *SCIENTIA SINICA Informatics*, 2024.

Belkhale, S. and Sadigh, D. Minivla: A better vla with a smaller footprint, 2024. URL <https://github.com/Stanford-ILIAD/openvla-mini>.

Bjorck, J., Castañeda, F., Cherniadev, N., Da, X., Ding, R., Fan, L., Fang, Y., Fox, D., Hu, F., Huang, S., et al. Gr00tn1: An open foundation model for generalist humanoid robots. *arXiv preprint arXiv:2503.14734*, 2025.

Black, K., Brown, N., Driess, D., Esmail, A., Equi, M., Finn, C., Fusai, N., Groom, L., Hausman, K., Ichter, B., et al. pi0: A vision-language-action flow model for general robot control. *arXiv preprint arXiv:2410.24164*, 2024.

Bu, Q., Yang, Y., Cai, J., Gao, S., Ren, G., Yao, M., Luo, P., and Li, H. Univla: Learning to act anywhere with task-centric latent actions. *arXiv preprint arXiv:2505.06111*, 2025.

Cadene, R., Alibert, S., Soare, A., Gallouedec, Q., Zouitine, A., Palma, S., Kooijmans, P., Aractingi, M., Shukor, M., Aubakirova, D., Russi, M., Capuano, F., Pascal, C., Choghari, J., Moss, J., and Wolf, T. Lerobot: State-of-the-art machine learning for real-world robotics in pytorch. <https://github.com/huggingface/lerobot>, 2024.

Chi, C., Xu, Z., Feng, S., Cousineau, E., Du, Y., Burchfiel, B., Tedrake, R., and Song, S. Diffusion policy: Visuomotor policy learning via action diffusion. *The International Journal of Robotics Research*, pp. 02783649241273668, 2023.

Dao, T. Flashattention-2: Faster attention with better parallelism and work partitioning. In *The Twelfth International Conference on Learning Representations*, 2024.

Dong, Z., Liu, Y., Li, Y., Zhao, H., and HAO, J. Conditioning matters: Training diffusion policies is faster than you think. In *The Thirty-ninth Annual Conference on Neural Information Processing Systems*, 2025.

Driess, D., Xia, F., Sajjadi, M. S., Lynch, C., Chowdhery, A., Ichter, B., Wahid, A., Tompson, J., Vuong, Q., Yu, T., et al. Palm-e: An embodied multimodal language model. *arXiv preprint arXiv:2303.03378*, 2023.

Driess, D., Springenberg, J. T., Ichter, B., Yu, L., Li-Bell, A., Pertsch, K., Ren, A. Z., Walke, H., Vuong, Q., Shi, L. X., and Levine, S. Knowledge insulating vision-language-action models: Train fast, run fast, generalize better. *arXiv preprint arXiv:2505.23705*, 2025.

Goyal, A., Hadfield, H., Yang, X., Blukis, V., and Ramos, F. Vla-0: Building state-of-the-art vlas with zero modification. *arXiv preprint arXiv:2510.13054*, 2025.

Hancock, A. J., Wu, X., Zha, L., Russakovsky, O., and Majumdar, A. Actions as language: Fine-tuning vlm into vlas without catastrophic forgetting. *arXiv preprint arXiv:2509.22195*, 2025.

Intelligence, P., Amin, A., Aniceto, R., Balakrishna, A., Black, K., Conley, K., Connors, G., Darpinian, J., Dhabalia, K., DiCarlo, J., Driess, D., Equi, M., Esmail, A., Fang, Y., Finn, C., Glossop, C., Godden, T., Goryachev, I., Groom, L., Hancock, H., Hausman, K., Hussein, G., Ichter, B., Jakubczak, S., Jen, R., Jones, T., Katz, B., Ke, L., Kuchi, C., Lamb, M., LeBlanc, D., Levine, S., Li-Bell, A., Lu, Y., Mano, V., Mothukuri, M., Nair, S., Pertsch, K., Ren, A. Z., Sharma, C., Shi, L. X., Smith, L., Springenberg, J. T., Stachowicz, K., Stoeckle, W., Swerdlow, A., Tanner, J., Torne, M., Vuong, Q., Walling, A., Wang, H., Williams, B., Yoo, S., Yu, L., Zhilinsky, U., and Zhou, Z. $\pi_{0,6}^*$: a vla that learns from experience. *arXiv preprint arXiv:2511.14759*, 2025a.

Intelligence, P., Black, K., Brown, N., Darpinian, J., Dhabalia, K., Driess, D., Esmail, A., Equi, M., Finn, C., Fusai, N., et al. pi0.5: a vision-language-action model with open-world generalization. *arXiv preprint arXiv:2504.16054*, 2025b.

Jaegle, A., Gimeno, F., Brock, A., Zisserman, A., Vinyals, O., and Carreira, J. Perceiver: General perception with iterative attention. *arXiv preprint arXiv:2103.03206*, 2021.

Khazatsky, A., Pertsch, K., Nair, S., Balakrishna, A., Dasari, S., Karamcheti, S., Nasiriany, S., Srirama, M. K., Chen, L. Y., Ellis, K., Fagan, P. D., Hejna, J., Itkina, M., Lepert, M., Ma, Y. J., Miller, P. T., Wu, J., Belkhale, S., Dass, S., Ha, H., Jain, A., Lee, A., Lee, Y., Memmel, M., Park, S., Radosavovic, I., Wang, K., Zhan, A., Black, K., Chi, C.,

Hatch, K. B., Lin, S., Lu, J., Mercat, J., Rehman, A., Sanketi, P. R., Sharma, A., Simpson, C., Vuong, Q., Walke, H. R., Wulfe, B., Xiao, T., Yang, J. H., Yavary, A., Zhao, T. Z., Agia, C., Baijal, R., Castro, M. G., Chen, D., Chen, Q., Chung, T., Drake, J., Foster, E. P., Gao, J., Herrera, D. A., Heo, M., Hsu, K., Hu, J., Jackson, D., Le, C., Li, Y., Lin, X., Ma, Z., Maddukuri, A., Mirchandani, S., Morton, D., Nguyen, T. K., O’Neill, A., Scalise, R., Seale, D., Son, V., Tian, S., Tran, E., Wang, A. E., Wu, Y., Xie, A., Yang, J., Yin, P., Zhang, Y., Bastani, O., Berseth, G., Bohg, J., Goldberg, K., Gupta, A., Gupta, A., Jayaraman, D., Lim, J. J., Malik, J., Martín-Martín, R., Ramamoorthy, S., Sadigh, D., Song, S., Wu, J., Yip, M. C., Zhu, Y., Kollar, T., Levine, S., and Finn, C. DROID: A large-scale in-the-wild robot manipulation dataset. In *RSS 2024 Workshop: Data Generation for Robotics*, 2024.

Kim, M. J., Pertsch, K., Karamcheti, S., Xiao, T., Balakrishna, A., Nair, S., Rafailov, R., Foster, E. P., Sanketi, P. R., Vuong, Q., Kollar, T., Burchfiel, B., Tedrake, R., Sadigh, D., Levine, S., Liang, P., and Finn, C. OpenVLA: An open-source vision-language-action model. In *8th Annual Conference on Robot Learning*, 2024.

Kim, M. J., Finn, C., and Liang, P. Fine-tuning vision-language-action models: Optimizing speed and success. *arXiv preprint arXiv:2502.19645*, 2025.

Lee, D., Kim, C., Kim, S., Cho, M., and Han, W.-S. Autoregressive image generation using residual quantization. In *Proceedings of the IEEE/CVF Conference on Computer Vision and Pattern Recognition, CVPR*, 2022.

Lee, J., Duan, J., Fang, H., Deng, Y., Liu, S., Li, B., Fang, B., Zhang, J., Wang, Y. R., Lee, S., Han, W., Pumacay, W., Wu, A., Hendrix, R., Farley, K., VanderBilt, E., Farhadi, A., Fox, D., and Krishna, R. Molmoact: Action reasoning models that can reason in space. *arXiv preprint arXiv:2508.07917*, 2025.

Lee, S., Wang, Y., Etukuru, H., Kim, H. J., Shafiullah, N. M. M., and Pinto, L. Behavior generation with latent actions. In *Forty-first International Conference on Machine Learning*, 2024.

Li, X., Hsu, K., Gu, J., Mees, O., Pertsch, K., Walke, H. R., Fu, C., Lunawat, I., Sieh, I., Kirmani, S., Levine, S., Wu, J., Finn, C., Su, H., Vuong, Q., and Xiao, T. Evaluating real-world robot manipulation policies in simulation. In *8th Annual Conference on Robot Learning*, 2024.

Liu, B., Zhu, Y., Gao, C., Feng, Y., Liu, Q., Zhu, Y., and Stone, P. Libero: Benchmarking knowledge transfer for lifelong robot learning. *Advances in Neural Information Processing Systems*, 36, 2024.

Liu, Y., Zhang, S., Dong, Z., Ye, B., Yuan, T., Yu, X., Yin, L., Lu, C., Shi, J., Yu, L. J.-T., Zheng, L., Jiang, T., Gong, J., Qiu, X., and Zhao, H. Faster: Toward efficient autoregressive vision language action modeling via neural action tokenization. *arXiv preprint arXiv:2512.04952*, 2025.

Marafioti, A., Zohar, O., Farré, M., noyan, M., Bakouch, E., Jiménez, P. M. C., Zakka, C., allal, L. B., Lozhkov, A., Tazi, N., Srivastav, V., Lochner, J., Larcher, H., Morlon, M., Tunstall, L., Werra, L. V., and Wolf, T. SmolVLM: Redefining small and efficient multimodal models. In *Second Conference on Language Modeling*, 2025.

Mees, O., Ghosh, D., Pertsch, K., Black, K., Walke, H. R., Dasari, S., Hejna, J., Kreiman, T., Xu, C., Luo, J., Tan, Y. L., Sadigh, D., Finn, C., and Levine, S. Octo: An open-source generalist robot policy. In *First Workshop on Vision-Language Models for Navigation and Manipulation at ICRA 2024*, 2024.

Mete, A., Xue, H., Wilcox, A., Chen, Y., and Garg, A. QueST: Self-supervised skill abstractions for learning continuous control. In *The Thirty-eighth Annual Conference on Neural Information Processing Systems*, 2024.

Pertsch, K., Stachowicz, K., Ichter, B., Driess, D., Nair, S., Vuong, Q., Mees, O., Finn, C., and Levine, S. Fast: Efficient action tokenization for vision-language-action models. *arXiv preprint arXiv:2501.09747*, 2025.

Qu, D., Song, H., Chen, Q., Yao, Y., Ye, X., Ding, Y., Wang, Z., Gu, J., Zhao, B., Wang, D., et al. Spatialvla: Exploring spatial representations for visual-language-action model. *arXiv preprint arXiv:2501.15830*, 2025.

Shukor, M., Aubakirova, D., Capuano, F., Kooijmans, P., Palma, S., Zouitine, A., Aractingi, M., Pascal, C., Russi, M., Marafioti, A., Alibert, S., Cord, M., Wolf, T., and Cadene, R. Smolvla: A vision-language-action model for affordable and efficient robotics. *arXiv preprint arXiv:2506.01844*, 2025.

van den Oord, A., Vinyals, O., and kavukcuoglu, k. Neural discrete representation learning. In *Advances in Neural Information Processing Systems*, 2017.

van den Oord, A., Li, Y., and Vinyals, O. Representation learning with contrastive predictive coding. *arXiv preprint arXiv:1807.03748*, 2019.

Walke, H. R., Black, K., Zhao, T. Z., Vuong, Q., Zheng, C., Hansen-Estruch, P., He, A. W., Myers, V., Kim, M. J., Du, M., et al. Bridgedata v2: A dataset for robot learning at scale. In *Conference on Robot Learning*, pp. 1723–1736. PMLR, 2023.

Wang, W., Gao, Z., Gu, L., Pu, H., Cui, L., Wei, X., Liu, Z., Jing, L., Ye, S., Shao, J., et al. Internvl3. 5: Advancing open-source multimodal models in versatility, reasoning, and efficiency. *arXiv preprint arXiv:2508.18265*, 2025a.

Wang, Y., Zhu, H., Liu, M., Yang, J., Fang, H.-S., and He, T. Vq-vla: Improving vision-language-action models via scaling vector-quantized action tokenizers. In *Proceedings of the IEEE/CVF International Conference on Computer Vision*, 2025b.

Yang, Q. T. A., Yang, B., Zhang, B., Hui, B., Zheng, B., Yu, B., Li, C., Liu, D., Huang, F., Wei, H., Lin, H., Yang, J., Tu, J., Zhang, J., Yang, J., Yang, J., Zhou, J., Lin, J., Dang, K., Lu, K., Bao, K., Yang, K., Yu, L., Li, M., Xue, M., Zhang, P., Zhu, Q., Men, R., Lin, R., Li, T., Tang, T., Xia, T., Ren, X., Ren, X., Fan, Y., Su, Y., Zhang, Y., Wan, Y., Liu, Y., Cui, Z., Zhang, Z., and Qiu, Z. Qwen2.5 technical report. *arXiv preprint arXiv:2412.15115*, 2025.

Zhang, S., Xu, Z., Liu, P., Yu, X., Li, Y., Gao, Q., Fei, Z., Yin, Z., Wu, Z., Jiang, Y.-G., et al. Vlabench: A large-scale benchmark for language-conditioned robotics manipulation with long-horizon reasoning tasks. In *Proceedings of the IEEE/CVF International Conference on Computer Vision*, pp. 11142–11152, 2025.

Zitkovich, B., Yu, T., Xu, S., Xu, P., Xiao, T., Xia, F., Wu, J., Wohlhart, P., Welker, S., Wahid, A., Vuong, Q., Vanhoucke, V., Tran, H., Soricut, R., Singh, A., Singh, J., Sermanet, P., Sanketi, P. R., Salazar, G., Ryoo, M. S., Reymann, K., Rao, K., Pertsch, K., Mordatch, I., Michalewski, H., Lu, Y., Levine, S., Lee, L., Lee, T.-W. E., Leal, I., Kuang, Y., Kalashnikov, D., Julian, R., Joshi, N. J., Irpan, A., brian ichter, Hsu, J., Herzog, A., Hausman, K., Gopalakrishnan, K., Fu, C., Florence, P., Finn, C., Dubey, K. A., Driess, D., Ding, T., Choromanski, K. M., Chen, X., Chebotar, Y., Carbajal, J., Brown, N., Brohan, A., Arenas, M. G., and Han, K. RT-2: Vision-language-action models transfer web knowledge to robotic control. In *7th Annual Conference on Robot Learning*, 2023.

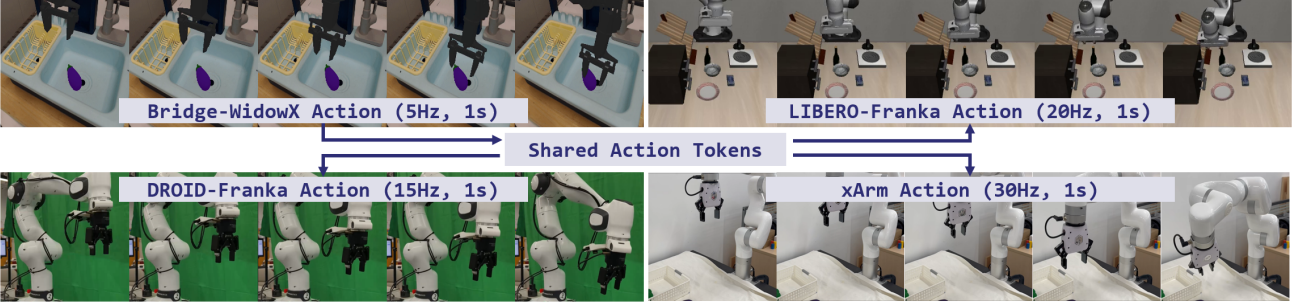


Figure 10. Cross-embodiment action transfer. To evaluate the transferability of ActionCodec, a 1-second WidowX action sequence sampled from BridgeData is encoded into action tokens and subsequently decoded into 1-second trajectories for LIBERO-Franka, DROID-Franka, and xArm. After deploying these sequences twice (totaling 2 seconds) and recording the resulting motions, all three robotic platforms exhibit highly consistent action patterns. This demonstrates that ActionCodec effectively captures hardware-agnostic action semantics.

A. Experimental Setup and Benchmark Details

A.1. Benchmarks

LIBERO. The LIBERO benchmark (Liu et al., 2024) comprises four task suites: *Goal*, *Spatial*, *Object*, and *Long*. Each suite contains 10 tasks, with 50 demonstrations provided per task. These suites evaluate the model’s performance in instruction following, spatial reasoning, object recognition, and long-horizon task completion. Following the official π_0 fine-tuning recipe, we fine-tune the VLM under a multi-task joint training setting for 30k steps. Evaluation is conducted over 50 trials per task using the predefined initial states.

SimplerEnv-WidowX. To assess zero-shot generalization, we utilize SimplerEnv-WidowX (Li et al., 2024), which provides four out-of-domain desktop manipulation tasks not included in the BridgeData set. We fine-tune the VLM on BridgeData for 4 epochs before direct evaluation. To mitigate the high variance typical of zero-shot evaluation, we increase the number of trials per task from the default 24 to 120.

SO100-ShapeSorter. We conduct real-world evaluations using the SO100 platform in a shape-sorting task. The robot must identify a specific numerical block (1–10) based on language instructions and insert it into the matching slot. The SO100 robotic arms were assembled according to the official LeRobot (Cadene et al., 2024) documentation³. Two 480x640 RGB cameras are utilized, mounted on the gripper and directly overhead, respectively. Data collection is performed at a frequency of 30Hz. Both proprioception and action spaces are defined by absolute joint angles. This benchmark tests both semantic recognition and fine-grained manipulation. We collect 50 demonstrations per block and fine-tune the VLM for 30k steps. During testing, block positions are randomized, and 20 trials are performed for each number. We record task progress at two checkpoints: 50% for a successful grasp and 100% for successful insertion. In Section 6.3, we distinguish between two variants: *w/ co-training* refers to ActionCodec trained on LIBERO (Liu et al., 2024), BridgeData (Walke et al., 2023), DROID (Khazatsky et al., 2024), the SO100-community dataset (Shukor et al., 2025), and the SO100-ShapeSorter dataset; *w/o co-training* excludes the SO100-community dataset. Detailed `repo_ids` for the community dataset are available in Shukor et al. (2025) Appendix A.1.

xArm-PickVeg. This benchmark involves a multi-task vegetable picking task where the xArm robot identifies and grasps a target vegetable model based on language instructions. The system uses only RGB images from a third-person Intel Realsense L515 camera, with data acquisition at 30Hz. Proprioception utilizes the end-effector (EEF) pose, while the action space is defined by delta EEF poses. We collect 30 demonstrations for each vegetable and fine-tune the VLM for 30k steps. During testing, object positions are randomized, and 20 trials are performed for each item. We utilize a binary success metric, as most failures are concentrated in the recognition or initial grasping phase. In Section 6.3, we denote the variant initialized with weights pre-trained on LIBERO, BridgeData, and DROID as *w/ PT*, while *w/o PT* refers to a randomly initialized model trained solely on the xArm dataset.

³Official SO100 document: <https://huggingface.co/docs/lerobot/s0100>

A.2. Details of Validation Experiments

To rigorously evaluate the design desiderata discussed in Section 4, we provide comprehensive details of our validation experimental setup.

VQ Tokenizer Architecture. As illustrated in Figure 2, we implement the encoder and decoder using a Perceiver-based Transformer architecture (Jaegle et al., 2021). This design provides the structural flexibility required for our ablation studies: utilizing only cross-attention layers ensures that action tokens remain mutually independent, while the integration of an auxiliary self-attention layer (with either bidirectional or causal masking) allows for the precise modulation of inter-token dependencies. This modularity is essential for our analysis of *residual grammar* in Section 4.3. While alternative backbones such as CNNs (Lee et al., 2024; Belkhale & Sadigh, 2024; Wang et al., 2025b) or standard Transformers (Liu et al., 2025) are prevalent in literature, we treat the specific choice of backbone as an orthogonal engineering consideration and focus primarily on the inherent properties of the tokenization scheme.

VLA Implementation. To isolate the influence of the action tokenizer, we adhere to a native VLM-style autoregressive paradigm. We perform full-parameter fine-tuning on SmolVLM2-256M (Marafioti et al., 2025) to predict action tokens without any robotics-specific architectural modifications (Table 6). This model scale is chosen for its competitive multimodal performance and computational tractability for extensive ablation studies. Specifically, we expand the VLM vocabulary with S special tokens: $\langle | \text{action}_0 | \rangle \dots \langle | \text{action}_{(S-1)} | \rangle$. During inference, any invalid token sequence produced by the VLM is substituted with a zero-action chunk to maintain control stability. For clarity, the [BOS] notation used in our analysis refers to the context token immediately preceding the action sequence in the prompt (see Section A.3), serving as a functional beginning-of-sentence marker for the action expert.

Notably, the **FAST tokenizer** (Pertsch et al., 2025) requires a specialized sequence-length alignment heuristic. Since FAST necessitates that the BPE-decoded sequence matches a specific length for valid reconstruction—a constraint frequently violated by autoregressive VLMs—we implement a soft-decoding approach involving zero-padding or truncation to the required length. Without this adjustment, models trained with FAST exhibit negligible success rates throughout the majority of the training phase.

Datasets and Benchmarking. While the action tokenizers are pre-trained on the comprehensive LIBERO dataset (Liu et al., 2024), VLA fine-tuning and evaluation are conducted specifically on the LIBERO-Goal task suite. We monitor performance at 500, 1k, 5k, 10k, and 20k training steps. We observe that performance below 500 steps is indistinguishable across variants, while models typically reach asymptotic convergence by 20k steps, providing a complete window into the training dynamics of each tokenization scheme.

A.2.1. IMPACTS OF OVERLAP RATE

In Section 4.1, we synthesize three tokenizer variants with controlled OR levels: 26%, 40%, and 70%. This controlled variance is achieved by augmenting the standard VQ-VAE objective function with an auxiliary InfoNCE contrastive loss (van den Oord et al., 2019): $\mathcal{L}_{\text{VQ}} + \lambda \cdot \mathcal{L}_{\text{InfoNCE}}$, where λ is a weighting hyperparameter that modulates the degree of latent clustering. For a given action sample A , we define a positive pair as the latent representation $Z = \mathcal{F}(A)$ and the representation of its perturbed version $Z^+ = \mathcal{F}(A + \eta)$, $\eta \sim \mathcal{N}(0, \sigma^2)$. All other action latents within the same mini-batch serve as negative samples Z^- . By minimizing the distance between Z and Z^+ in the latent manifold, we implicitly increase the probability that semantically similar actions are mapped to the same discrete code, thereby elevating the OR. Our experiments reveal that a higher overlap rate significantly enhances the training efficiency of the VLA model. However, in subsequent validation experiments, we observe that incorporating a *Time Contrastive Loss* (TCL) or a *CLIP-style* cross-modal loss (Section 4.3) naturally yields higher OR values while providing superior training stability compared to the explicit InfoNCE-based action perturbation. Consequently, our final architecture favors these more stable contrastive objectives.

A.2.2. IMPACTS OF RESIDUAL GRAMMAR

In Section 4.3, we analyze the impact of *residual grammar* on VLA training by comparing three tokenizer variants: **Independent**, **SA** (Self-Attention), and **Causal**. These variants are implemented by modifying the internal architecture of the Perceiver network. As shown in Figure 11, the network structure using only cross-attention layers (**Independent**) ensures that each learnable embedding interacts exclusively with the input sequence. Consequently, the resulting output tokens lack explicit inter-dependencies. By introducing an additional self-attention layer, the learnable embeddings interact with each other; specifically, we can employ either bidirectional attention (**SA**) or causal masking (**Causal**) to alter the

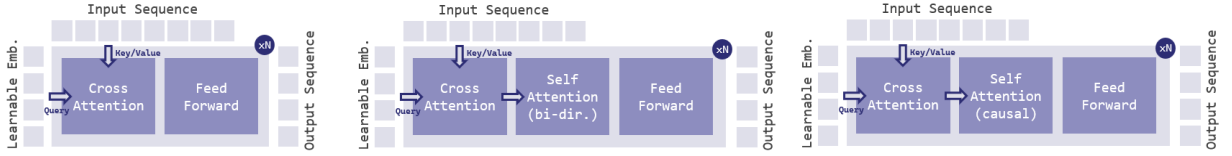


Figure 11. Comparison of Perceiver architectures for Residual Grammar: (left) Independent (cross-attention only), (middle) SA (with self-attention), and (right) Causal (with causal self-attention)

Table 6. VLA Training Hyperparameters. Detailed configurations for the validation experiments on LIBERO-Goal.

Hyperparameters	Values
GPUs	8×NVIDIA RTX 3090 (24 GB VRAM)
Learning Rate	2×10^{-4} peak (1k steps linear warmup, 30k steps cosine decay to 2×10^{-5})
Global Batch Size	128 (16 per GPU)
Training Steps	30k (LIBERO-Goal only)
Input Modalities	1× Third-person camera, 1× Wrist camera (concatenated)
Input Image Size	224 × 448
Use Proprioception	True
Image Augmentation	Random crop (87.5%), Brightness/Contrast/Saturation (0.2), Hue (0.05)

dependency relationships between the output tokens.

To specifically analyze the impact of these variants on VLA training, we design a **perturbation experiment** in Figure 6. The procedure is as follows: we sample vision-language-action tuples (V, L, A) from the dataset and provide V and L as inputs to the trained VLA model to predict action tokens. During the autoregressive prediction process, we randomly shuffle the token at a specific position. The model then continues to predict the remaining tokens. Finally, the predicted action tokens are decoded into a predicted action \hat{A} , and we calculate the L_1 distance between the ground truth A and the predicted \hat{A} . Our results show that the **Independent** variant maintains a stable and lower error compared to the **SA** and **Causal** architectures. This indicates that VLA performance using SA (full dependency) or Causal (temporal dependency) is inferior to the Independent variant. This is attributed to the fact that when predicting action tokens, the VLA model becomes overly reliant on preceding tokens, leading to reduced robustness.

A.3. Details of Tokenizer Comparison Experiments

Action Tokenizers. We evaluate the ActionCodec models introduced in Section 5, pre-trained on LIBERO (Liu et al., 2024), BridgeData (Walke et al., 2023), and DROID (Khazatsky et al., 2024). Training utilized a batch size of 8,192 and a learning rate of 2×10^{-4} for 100k steps. Following the FAST tokenizer (Pertsch et al., 2025), our tokenizer encodes a fixed temporal window of 1 second. To accommodate heterogeneous control frequencies across datasets, we employ timestamp-based positional encodings to ensure temporal awareness.

For baselines, we implement several mainstream schemes: (i) **Binning** (Goyal et al., 2025): Each action dimension is discretized into 1,000 bins. Due to its linear token growth relative to action dimensionality and horizon, a 1-second window (20Hz) would result in a prohibitive 140 tokens per chunk for 7-DoF LIBERO tasks; thus, we constrain its horizon to $T = 8$. (ii) **String** (Hancock et al., 2025): Actions are represented as raw Python list strings. Since this representation incurs an even higher token budget depending on precision and BPE encoding, we similarly adopt $T = 8$ to maintain training tractability. (iii) **VQ-baselines**: We utilize official implementations⁴ and checkpoints for MiniVLA (Belkhale & Sadigh, 2024) and VQ-VLA (Wang et al., 2025b) after aligning data statistics. (iv) **FAST**: We utilize the officially released universal version (Pertsch et al., 2025)⁶.

VLA Implementation. Consistent with our validation experiments, all tokenizers are evaluated using a SmolVLM2-2.2B backbone without structural modifications. We perform full-parameter autoregressive fine-tuning; specific hyperparameters are summarized in Table 7.

⁴MiniVLA: <https://github.com/Stanford-ILIAD/openvla-mini>

⁵VQVLA: <https://github.com/xiaoxiao0406/VQ-VLA>

⁶FAST: <https://huggingface.co/physical-intelligence/fast>

Table 7. VLA Training Hyperparameters. Detailed configurations for the tokenizer comparison experiments on LIBERO.

Hyperparameters	Values
GPUs	4×NVIDIA A100 (80 GB VRAM)
Learning Rate	10^{-4} peak (1k steps linear warmup, 30k steps cosine decay to 10^{-5})
Global Batch Size	128 (32 per GPU)
Training Steps	30k (applied to all four LIBERO task suites)
Input Modalities	1× Third-person camera, 1× Wrist camera (concatenated)
Input Image Size	224 × 448
Use Proprioception	True
Image Augmentation	Random crop (87.5%), Brightness/Contrast/Saturation (0.2), Hue (0.05)

Table 8. VLA Training Hyperparameters. Detailed configurations for the Simpler-WidowX experiments.

Hyperparameters	Values
GPUs	8×NVIDIA H100 (94 GB VRAM)
Learning Rate	2×10^{-5}
Global Batch Size	128 (16 per GPU)
Training Epochs	4
Input Modalities	1× Third-person camera
Input Image Size	224 × 224
Use Proprioception	True
Image Augmentation	Random crop (90%), Brightness/Contrast/Saturation (0.2), Hue (0.05)

Table 9. VLA Training Hyperparameters. Detailed configurations for the real-world experiments on SO100 and xArm.

Hyperparameters	Values
GPUs	4×NVIDIA A100 (80 GB VRAM)
Learning Rate	5×10^{-5} peak (1k steps linear warmup, 30k steps cosine decay to 5×10^{-6})
Global Batch Size	64 (16 per GPU)
Training Steps	30k
Input Modalities	SO100: 1× Third-person camera, 1× Wrist camera (concatenated), xArm: 1× Third-person camera
Input Image Size	224×448 for SO100, 224×224 for xArm
Use Proprioception	True
Image Augmentation	Brightness/Contrast/Saturation (0.2), Hue (0.05)

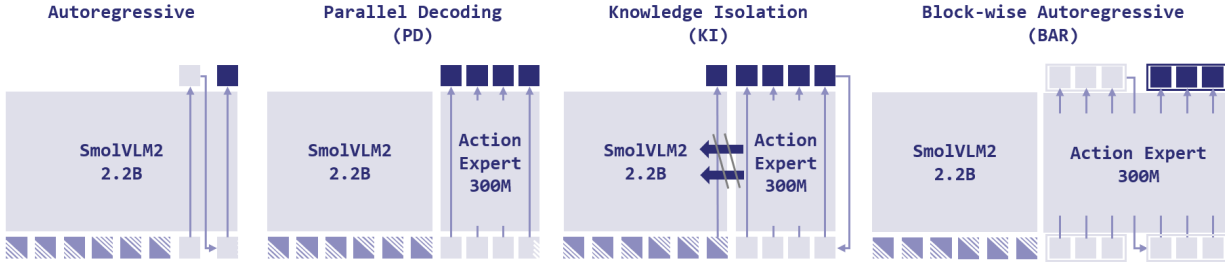


Figure 12. VLA paradigm architectures.

Datasets and Benchmarking. A single VLA model is trained across all LIBERO task suites simultaneously. We observe empirical convergence for all variants by 30k steps, beyond which performance gains become negligible. Following the official LIBERO evaluation protocol, we report results based on 50 trials per task, initialized from the 50 predefined environment states.

Prompt for VLM

```
[  
  {  
    "role": "system",  
    "content": "Analyze the input image and predict robot actions."  
  },  
  {  
    "role": "user",  
    "content": [  
      {"type": "image"},  
      {  
        "type": "text",  
        "text": "**State**: {state}, **Task**: {task}."  
      }  
    ]  
  },  
  {  
    "role": "assistant",  
    "content": [  
      {  
        "type": "text",  
        "text": "{action}: <|action_n|> ... <|action_m|>"  
      }  
    ]  
  ]  
]
```

A.4. Details of Paradigm Adaptation Experiments

In Section 6.2, we explore the compatibility of **ActionCodec** with three prevailing VLA paradigms. Since each paradigm requires a specialized attention mask design for action tokens, it often prevents the VLM backbone from utilizing *Flash Attention* (Dao, 2024), which significantly degrades training efficiency. To circumvent this, following the architecture of π_0 (Black et al., 2024), we introduce a 300M-parameter **action expert** to handle action token prediction. This expert receives the KV cache from the VLM backbone and employs independent feed-forward layers. We provide the architecture in Figure 12 and the implementation details are as follows:

Parallel Decoding (PD). The action expert utilizes bidirectional attention and takes n learnable [BOS] tokens as input to directly predict the logits of n action tokens in a single forward pass. During inference, we perform a simple *argmax* on the logits to obtain tokens. We observed that *argmax* yields performance comparable to probabilistic sampling, likely because ActionCodec produces highly condensed semantic information with naturally low perplexity. Furthermore, PD achieves success rates similar to naive autoregression. This can be attributed to the token independence of ActionCodec,

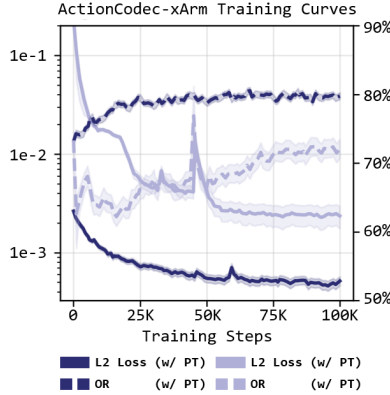


Figure 13. Learning curves of ActionCodec with and without pre-training. Compared to random initialization, initializing with pre-trained ActionCodec weights and fine-tuning on novel robotic data results in significantly lower L2 loss (higher reconstruction accuracy) and a higher Overlap Rate (OR). These results demonstrate that the pre-trained ActionCodec possesses a unified and semantically rich latent space, enabling rapid adaptation to new robotic action patterns.

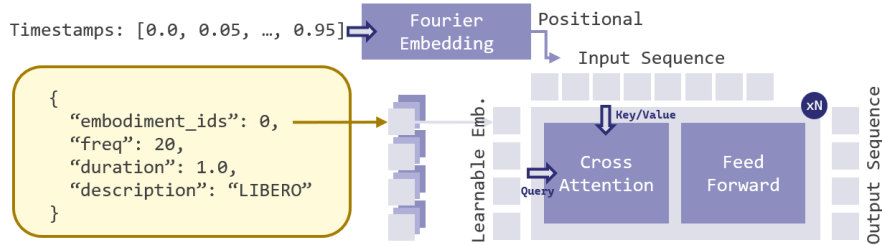


Figure 14. Illustration of the Soft-Prompt integration within the Perceiver architecture. Learnable embeddings represent embodiment IDs, while fourier embeddings provide temporal grounding for varying control frequencies.

which makes modeling inter-token correlations via autoregression redundant. Compared to naive autoregression (requiring n forward passes), PD significantly reduces inference latency by requiring only one.

Knowledge Isolation (KI). The action expert is implemented as a bidirectional attention network within a *flow-matching* framework. It takes noisy actions, denoising timestamps, and the VLM’s KV cache as input to predict the velocity field. During training, both the VLM’s autoregressive loss and the expert’s flow-matching loss are optimized simultaneously, though the gradient flow from the expert to the VLM is severed. While the performance of this KI variant is slightly lower than the naive autoregressive baseline, it remains superior to KI training using the FAST tokenizer. This suggests that while ActionCodec is highly effective, the KI paradigm may be better suited for large-scale VLA pre-training, where the VLM can be enriched with broad robotic priors, rather than fine-tuning on specific benchmarks.

Block-wise Autoregressive (BAR). The action expert utilizes a block-wise causal mask, where tokens within the same block are mutually visible, while blocks can only attend to preceding blocks. Each block corresponds to tokens from a single level of the RVQ codebooks. Due to the residual nature of RVQ, BAR with a single forward pass is equivalent to PD. Additional passes iteratively refine prediction accuracy; even if initial predictions are noisy, the error-damping property of the residual structure ensures stability. In our experiments, the BAR variant achieved the highest performance, establishing a new **SOTA** on the LIBERO benchmark for models without robotics-specific pre-training.

B. Details of Soft-Prompt

In Section 5, we employ a **soft-prompt** mechanism to facilitate multi-embodiment data integration and cross-platform knowledge transfer. This approach is highly compatible with the **Perceiver** architecture, as the Perceiver fundamentally requires learnable embeddings to serve as the input for the query side of the Transformer-based network. Specifically, as shown in Figure 14, we have configured information for all embodiments included in the pre-training dataset, documenting their respective control frequencies, the action durations encoded by the tokenizer, and their unique indices. We assign

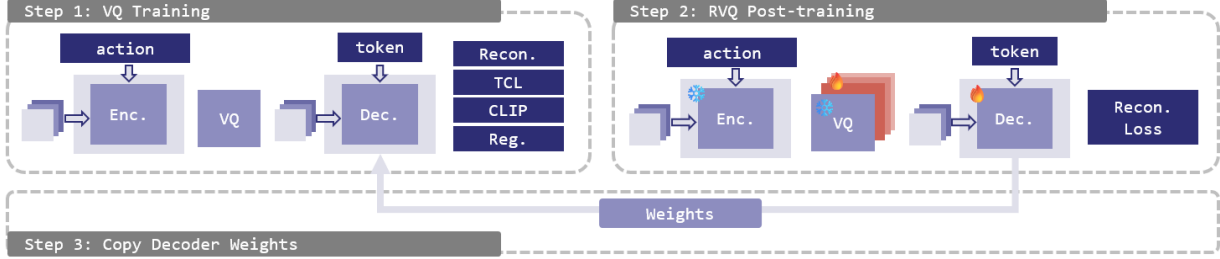


Figure 15. Procedure of RVQ post-training.

a dedicated learnable embedding to each embodiment index. For the input components involving action timestamps, specifically the key/value inputs of the encoder and the query inputs of the decoder, we calculate the timestamp for each token based on the control frequency and action duration. These timestamps are then processed via fourier embedding to serve as positional encodings. This design ensures that our tokenizer can not only distinguish between different embodiments but also maintain a consistent temporal perception of motion across various platforms.

C. Details of RVQ Post-training

As discussed in Section 5, we find that RVQ post-training is an effective method for reducing reconstruction error at no additional cost while maintaining a high Overlap Rate (OR) and vision-language alignment. In our experimental setup, as shown in Figure 15, we first train a VQ-based ActionCodec with $n = 16$ tokens. We then initialize an RVQ variant with $n = 16$ and a residual depth of $L = 3$, inheriting the encoder and primary codebook weights from the VQ model and freezing them. Post-training is performed using only reconstruction loss and RVQ objectives. Since the encoder and the first codebook are frozen, the output tokens from the first codebook of the RVQ model remain identical to those produced by the original VQ version. By simply copying the post-trained RVQ decoder weights back to the VQ model, we enhance reconstruction fidelity without altering the action tokenization procedure. In our evaluations, ActionCodec-BAR utilizes the full RVQ tokenizer, whereas all other models employ the VQ-version tokenizer enhanced by the post-trained RVQ decoder.

D. Artifact Entropy on Deterministic Tokenization

To evaluate the topological stability of the discrete action space, we introduce the concept of *Artifact Entropy* in Section 4. While the Vector Quantized (VQ) encoder \mathcal{F} is mathematically deterministic, thereby implying $H(C|A) = 0$ for any fixed point A in the action manifold, this idealization fails to account for the stochastic nature of real-world robotic control. Consequently, we define Artifact Entropy under the assumption of local physical perturbations, formalizing the entropy of tokens induced by infinitesimal noise within the action space:

$$H(C|A) \triangleq \mathbb{E}_{\epsilon \sim \mathcal{N}(0, \sigma^2)}[H(\mathcal{F}(A + \epsilon))], \quad (7)$$

where ϵ represents high-frequency sensor noise or control jitter. This metric quantifies the sensitivity of the quantization boundaries. A high Artifact Entropy suggests that negligible fluctuations in the input signal can cause the tokenizer to oscillate between disparate discrete codes. Such behavior introduces significant aleatoric uncertainty into the Vision-Language-Action (VLA) model’s supervision signal. In practice, high values of $H(C|A)$ manifest as inconsistencies within the training dataset. To render this phenomenon trackable, we utilize the *Overlap Rate* (OR) of adjacent action sequences as an empirical proxy. Given that temporal neighbors in a trajectory typically correspond to nearly identical visual observations and identical language instructions, a high Artifact Entropy results in divergent token sequences for similar contexts.